

## Anisotropic transport properties in InAs/AlSb heterostructures

G. Moschetti,<sup>a)</sup> H. Zhao, P.-Å. Nilsson, S. Wang, A. Kalabukhov, G. Dambrine,<sup>b)</sup> S. Bollaert,<sup>b)</sup> L. Desplanque,<sup>b)</sup> X. Wallart,<sup>b)</sup> and J. Grahn

Department of Microtechnology and Nanoscience (MC2), Microwave Electronics Laboratory, Chalmers University of Technology, SE-412 96 Göteborg, Sweden

(Received 15 November 2010; accepted 22 November 2010; published online 17 December 2010)

We have investigated the anisotropic transport behavior of InAs/AlSb heterostructures grown on a (001) InP substrate. An electrical analysis showed anisotropic sheet resistance  $R_{sh}$  and electron mobility  $\mu_n$  in the two dimensional electron gas (2DEG). Hall measurements demonstrated an enhanced anisotropy in  $\mu_n$  when cooled from room temperature to 2 K. High electron mobility transistors exhibited 27% higher maximum drain current  $I_{DS}$  and 23% higher peak transconductance  $g_m$  when oriented along the [1-10] direction. The anisotropic transport behavior in the 2DEG was correlated with an asymmetric dislocation pattern observed in the surface morphology and by cross-sectional microscopy analysis of the InAs/AlSb heterostructure. © 2010 American Institute of Physics. [doi:10.1063/1.3527971]

The InAs/AlSb High electron mobility transistor (HEMT) is a promising device candidate for microwave/millimeter-wave circuits because of a large conduction band offset between InAs and AlSb, high peak electron velocity, and high electron concentration in the InAs channel.<sup>1</sup> The main reason for the interest in this device technology is that the InAs/AlSb HEMT exhibits similar performance as the established InGaAs/InAlAs HEMT at one-fourth of its power dissipation.<sup>2</sup> However, because of the relatively large lattice constant of InAs, a 10–15 nm thick InAs channel must be grown on an InP or GaAs substrate only through the use of a thick (1–2  $\mu\text{m}$ ) relaxed AlSb metamorphic buffer.<sup>3</sup> This results in a tensile strain in the InAs channel with respect to the AlSb metamorphic buffer leading to the formation of threading dislocations.<sup>4</sup> Anisotropic electron transport in HEMT devices based on strained layers of III-V alloys has been reported earlier.<sup>5,6</sup> However, no anisotropy behavior in InAs/AlSb heterostructures has been reported so far. In this letter we report on a strong anisotropy in the electron transport and device performance observed for the InAs/AlSb HEMTs grown on a (001) InP substrate. Surface morphology characterization and cross-sectional scanning transmission electron microscopy (STEM) analysis showed the presence of elongated cracks along the [1-10] direction. These cracks were correlated with a 53% higher Hall  $\mu_n$  as well as with a 27% and 23% higher  $I_{DS}$  and peak  $g_m$ , respectively, along the [1-10] direction compared to the [110] direction.

The InAs/AlSb heterostructure was grown by molecular beam epitaxy on a 2 in. semi-insulating (001) InP substrate. The structure is equivalent to the one reported in Ref. 7 but with tellurium (Te) delta doping. A metamorphic buffer formed by AlSb (750 nm thick) and  $\text{Al}_{0.8}\text{Ga}_{0.2}\text{Sb}$  (250 nm thick) was grown over an  $\text{In}_{0.5}\text{Al}_{0.5}\text{As}$  smoothing layer on the (100) InP substrate. A 50 nm thick AlSb barrier and a 15 nm thick InAs channel were grown in order to form the active part together with a 5 nm AlSb spacer. A Te  $\delta$ -doping layer

with a nominal sheet density of  $4 \times 10^{12} \text{ cm}^{-2}$ , an 8 nm AlSb Schottky barrier, a 4 nm  $\text{In}_{0.5}\text{Al}_{0.5}\text{As}$  protection layer, and a 5 nm Si-doped InAs cap layer were then grown on top.

HEMTs with a 2  $\mu\text{m}$  gate length have been fabricated and characterized with the channel oriented along the three different directions ([1-10], [110], and [100]) in the InAs/AlSb heterostructure. The  $I_{DS}$  versus gate-source bias  $V_{GS}$  of adjacent HEMT devices oriented along the three directions is shown in Fig. 1 for a drain-source voltage  $V_{DS}$  of 0.5 V. The HEMT with the channel oriented along the [1-10] direction exhibits the highest maximum  $I_{DS}$  of 420 mA/mm at  $V_{GS} = 0$  V. In contrast, the maximum  $I_{DS}$  measured in the HEMT with the channel oriented along the [110] direction is instead 330 mA/mm. Furthermore, the HEMT with the channel oriented along the diagonal [100] direction shows a maximum  $I_{DS}$  of 375 mA/mm. Hence the maximum  $I_{DS}$  for the HEMT oriented along the [100] direction corresponds to a mean value of the two orthogonal directions. As a consequence, the  $g_m$  is also dependent on the HEMT channel orientation. In Fig. 2, the  $g_m$  of the HEMT devices is plotted versus  $V_{GS}$ ,

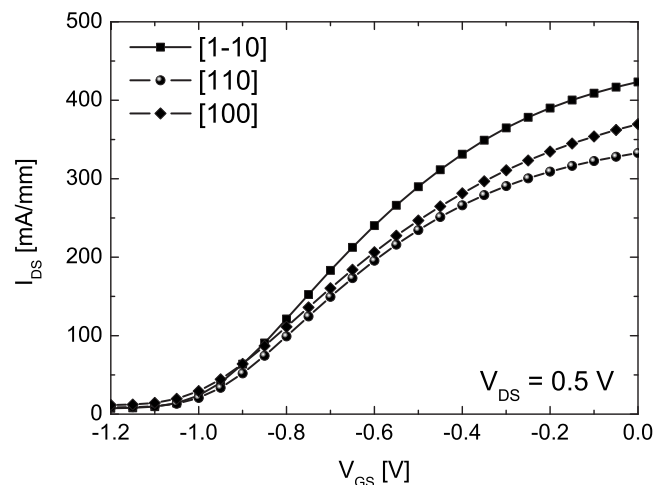


FIG. 1.  $I_{DS}(V_{GS})$  for InAs/AlSb HEMTs oriented along the [1-10] (squares), [110] (circles), and [100] (diamonds) directions. The device gate width is  $2 \times 50 \mu\text{m}$ , the gate length is 2  $\mu\text{m}$ , and the source-drain distance is 5.6  $\mu\text{m}$ .

<sup>a)</sup>Electronic mail: giuseppe.moschetti@chalmers.se.

<sup>b)</sup>Also at Institute of Electronics, Microelectronics and Nanotechnology, IEMN/CNRS UMR 8520, University Lille1, Av. Poincaré, 59652 Villeneuve d'Ascq, France.

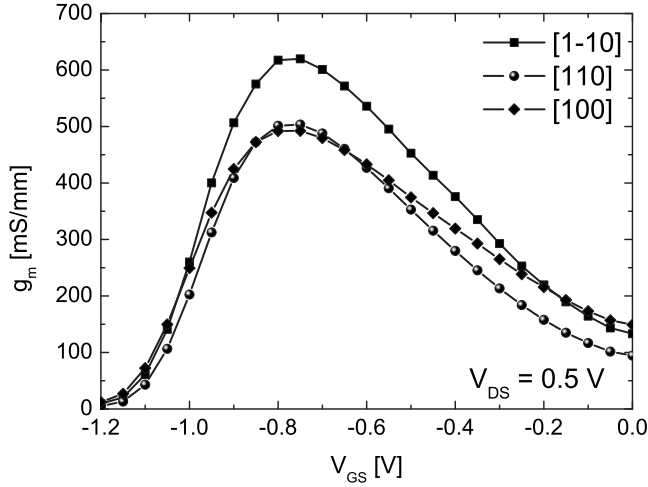


FIG. 2.  $g_m(V_{GS})$  for InAs/AlSb HEMTs oriented along the [1-10] (squares), [110] (circles), and [100] (diamonds) directions.

revealing a peak  $g_m$  about 23% higher along the [1-10] direction compared to the HEMTs oriented along the [110] direction. Thus the HEMT behavior in Figs. 1 and 2 indicates anisotropic transport in the two dimensional electron gas (2DEG).

In order to further investigate the transport properties along different orientations of the InAs/AlSb heterostructure, test structures such as transmission line model (TLM), van der Pauw, and Hall bars have been fabricated and characterized along the same three different orientations used for the HEMTs. TLM structures oriented along the two orthogonal directions [1-10] and [110], as well as TLM oriented at a 45° angle to the [1-10] direction ([100]), have been evaluated in order to determine the  $R_{sh}$  as a function of the orientation in the material. As seen in Table I, the TLM measurements showed a strong dependence in  $R_{sh}$  with the orientation of the wafer. The measured  $R_{sh}$  was  $118 \pm 0.5 \text{ } \Omega/\text{sq}$  along the direction [1-10], while a higher value of  $174 \pm 0.9 \text{ } \Omega/\text{sq}$  was observed along the direction [110]. An intermediate  $R_{sh}$  value of  $140 \pm 0.3 \text{ } \Omega/\text{sq}$  was measured along the diagonal direction [100]. The normalized contact resistance  $R_c$  extracted from the TLM measurements at different orientations showed a negligible orientation dependence. van der Pauw structures rotated at 45° have also been characterized, showing an  $R_{sh}$  value of  $143 \pm 1.3 \text{ } \Omega/\text{sq}$ . These results are in good agreement with the TLM oriented along the diagonal direction [100].

Hall bar test structures fabricated along the three different orientations were characterized from 300 to 2 K. The measured  $\mu_n$  and  $R_{sh}$  plotted versus temperature are shown in Fig. 3. Compared to the [110] direction, the  $\mu_n$  is higher along the [1-10] direction in the whole temperature range. This is hence in good agreement with the behavior of both HEMT devices and TLM structures. Furthermore, it is interesting to observe that the anisotropy in the mobility is en-

TABLE I.  $R_{sh}$  and  $R_c$  measured from TLM structures oriented along three different directions in the InAs/AlSb heterostructure.

TLM orientation	[1-10]	[110]	[100]
$R_{sh}$ ( $\Omega/\text{sq}$ )	$118 \pm 0.5$	$174 \pm 0.9$	$140 \pm 0.3$
$R_c$ ( $\Omega \text{ mm}$ )	$0.05 \pm 0.002$	$0.045 \pm 0.005$	$0.04 \pm 0.001$

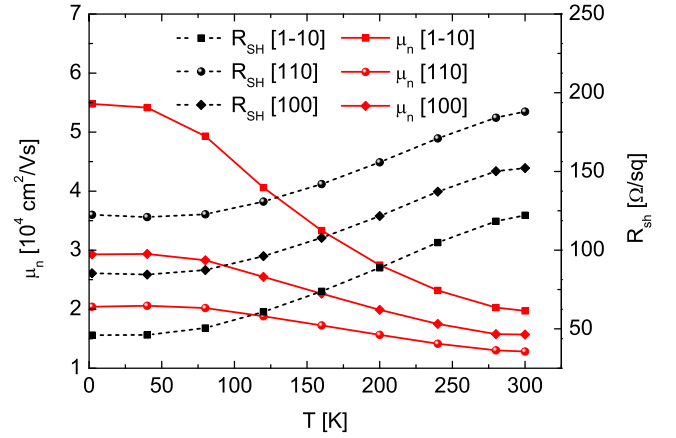


FIG. 3. (Color online)  $R_{sh}$  and  $\mu_n$  for InAs/AlSb Hall bar structures as a function of temperature for directions [1-10] (squares), [110] (circles), and [100] (diamonds).

hanced when reducing the temperature. Compared to 300 K,  $\mu_n$  at 2 K is 178% higher along the [1-10] direction and 59% higher along the [110] direction. Thus, at 2 K, the scattering of electrons occurring against the asymmetric cracks in the channel is the dominant mechanism. When increasing the temperature, the polar optical scattering<sup>8</sup> increases leading to a lower anisotropy in the mobility. The measured Hall sheet carrier density  $n_s$  shows instead a negligible dependence with the orientation and a small reduction of less than 5% at 2 K, compared to 300 K.

In order to clarify the origin of the anisotropic transport in the InAs/AlSb heterostructure, atomic force microscopy (AFM) has been carried out on the top InAs cap layer. As shown in Fig. 4, cracks elongated in the direction [1-10], with a terrace width of about 120 nm, are clearly visible on the InAs surface. This leads to surface roughnesses (rms) of 1.13 and 1.67 nm along the directions [1-10] and [110], respectively. As an initial thought, the presence of these cracks could be attributed to the tensile strain in the  $\text{In}_{0.5}\text{Al}_{0.5}\text{As}$  protection layer resulting from a large lattice mismatch compared with the relaxed AlSb Schottky barrier. In order to

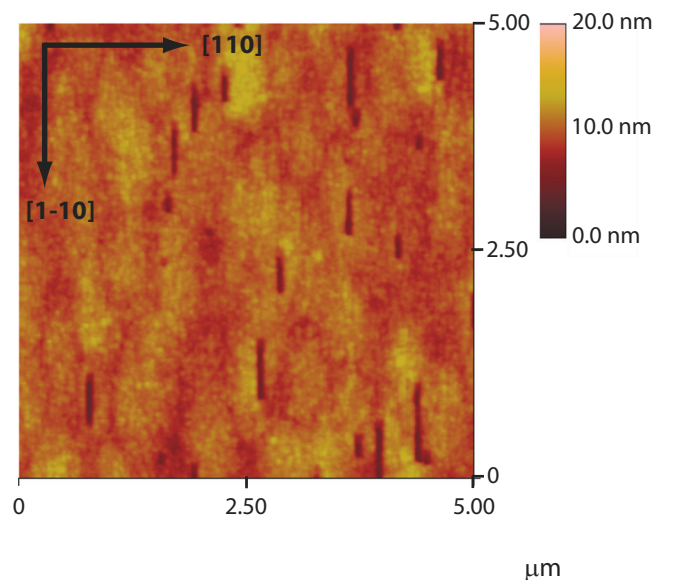


FIG. 4. (Color) AFM measurement ( $5 \times 5 \text{ } \mu\text{m}^2$ ) performed on top of the InAs cap layer of the InAs/AlSb heterostructure.

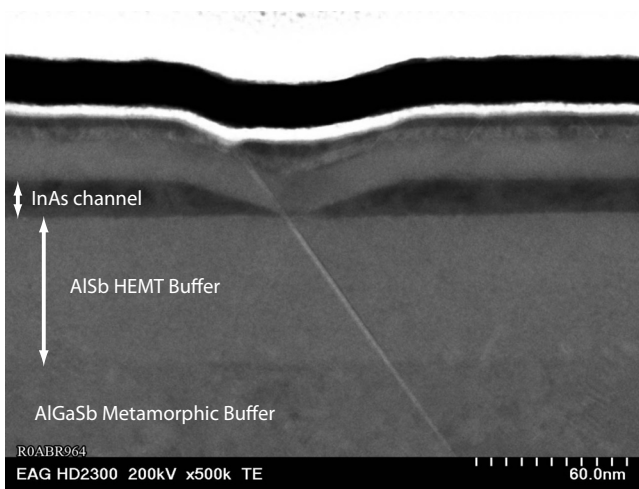


FIG. 5. STEM picture of the InAs/AISb HEMT cross-section cut along the [110] direction. The physical pinch of the channel caused by a threading dislocation originating from the metamorphic AISb/InP bulk interface is clearly visible.

investigate the origin of the elongated cracks, a STEM analysis has been performed on the InAs/AISb HEMT heterostructure. Figure 5 shows a STEM image of the structure cut along the [110] direction. The STEM analysis clearly shows that a threading dislocation propagates throughout the structure inducing a pit in the InAs channel. This results in depletion of the InAs layer around the threading dislocation leading to a crack observed from the AFM of the surface. Furthermore, a larger scale STEM image shows that there is always a threading dislocation connected with the bottom of each pit. From Fig. 5, the pit shows a symmetric shape along the [110] direction; However, its shape along the [1-10] direction is still unclear. Therefore, it may also be a crack in the InAs channel instead of a pit. Similar phenomena of such threading dislocation associated pits have also been found in the InGaN/GaN multiple quantum wells; the pit has a hexahedron cone shape and its formation is related to the local In diffusion around the dislocation core.<sup>9</sup> In order to clarify the origin of the anisotropic surface roughness and the crack direction, a structure formed by a 1  $\mu\text{m}$  thick AISb buffer was grown on top of a 100 nm thick  $\text{In}_{0.52}\text{Al}_{0.48}\text{As}$  layer on a semi-insulating (001) InP substrate. AFM measurements performed on top of the AISb layer showed anisotropic surface rms roughnesses of 0.73 and 1.596 nm along the directions [1-10] and [110], respectively. The anisotropic roughness observed in the AISb buffer is due to the anisotropy of the initial strain relaxation near the AISb/InAlAs/InP interface and of different diffusion lengths of adatoms along different crystallographic directions.<sup>10</sup>

The anisotropic electrical properties of the InAs/AISb HEMTs observed through HEMTs, TLM, and Hall bar measurements are closely related to the elongated cracks seen in the InAs/AISb heterostructure. It has been reported that scattering of electrons at charged dislocations reduces the transverse electron mobility.<sup>11</sup> A crack can be regarded as a dislocation array. Since the cracks are along the [1-10] direction, the scattering along the [110] direction is much larger than that along the [1-10] direction, resulting in a lower  $\mu_n$ .

In summary, we have investigated anisotropic transport phenomena occurring in InAs/AISb HEMTs grown on (001) InP substrates. TLM measurements showed a 32% lower  $R_{sh}$  along the [1-10] direction compared to the value along the [110] direction. Device measurements confirmed the anisotropy in the 2DEG with a 27% higher maximum  $I_{DS}$  and a 23% higher peak  $g_m$  for the HEMTs with the channel parallel to the [1-10] direction compared to the [110] direction. Hall bar structures showed that the anisotropy was enhanced when reducing the temperature, most likely due to the reduced polar optical scattering in the channel at low temperature. The anisotropic transport has been found to be related to the presence of threading dislocations in the AISb metamorphic buffer. This caused elongated cracks parallel to the [1-10] direction in the InAs channel.

This work was supported by the Swedish Research Council (VR) Grant No. 621-2009-4818. We are grateful to Martin Fagerlind at Chalmers for assistance and advice in the initial Hall transport measurements.

- <sup>1</sup>B. R. Bennett, R. Magno, J. B. Boos, W. Kruppa, and M. G. Ancona, *Solid-State Electron.* **49**, 1875 (2005).
- <sup>2</sup>B. Y. Ma, J. Bergman, P. Chen, J. B. Hacker, G. Sullivan, G. Nagy, and B. Brar, *IEEE Trans. Microwave Theory Tech.* **54**, 4448 (2006).
- <sup>3</sup>X. Wallart, J. Lastennet, D. Vignaud, and F. Mollot, *Appl. Phys. Lett.* **87**, 043504 (2005).
- <sup>4</sup>H.-R. Blank, M. Thomas, K. C. Wong, and H. Kroemer, *Appl. Phys. Lett.* **69**, 2080 (1996).
- <sup>5</sup>P. Hiesinger, T. Schweizer, K. Kohler, P. Ganser, W. Rothmund, and W. Jantz, *J. Appl. Phys.* **72**, 2941 (1992).
- <sup>6</sup>F. Peiró, J. C. Ferrer, A. Cornet, J. R. Morante, M. Beck, and M. A. Py, *Mater. Sci. Eng., B* **44**, 325 (1997).
- <sup>7</sup>G. Moschetti, P. A. Nilsson, N. Wadefalk, M. Malmkvist, E. Lefebvre, J. Grahn, Y. Roelens, A. Noudeviwa, A. Olivier, S. Bollaert, F. Danneville, L. Desplanque, X. Wallart, and G. Dambriane, in *IEEE International Conference on Indium Phosphide and Related Materials, IPRM '09*, 2009, p. 323.
- <sup>8</sup>K. Brennan and K. Hess, *Solid-State Electron.* **27**, 347 (1984).
- <sup>9</sup>Y. Chen, T. Takeuchi, H. Amano, I. Akasaki, N. Yamada, Y. Kaneko, and S. Y. Wang, *Appl. Phys. Lett.* **72**, 710 (1998).
- <sup>10</sup>H. Li, Q. Zhuang, Z. Wang, and T. Daniels-Race, *J. Appl. Phys.* **87**, 188 (2000).
- <sup>11</sup>N. G. Weimann, L. F. Eastman, D. Doppalapudi, H. M. Ng, and T. D. Moustakas, *J. Appl. Phys.* **83**, 3656 (1998).